

Mechanical Properties of x PMN-(1- x)PZT Ceramic Systems

Rattikorn Yimnirun*, Ekarat Meechoowas, Supon Ananta and Tawee Tunkasiri

Department of Physics, Faculty of Science, Chiang Mai University, Chiang Mai 50200, Thailand

*Corresponding author. E-mail: rattikor@chiangmai.ac.th

ABSTRACT

Most of earlier work on PMN-PZT ceramic systems has been mainly focused on processing and electrical properties, while knowledge on mechanical properties is scarce. This article describes for the first time mechanical properties of the PMN-PZT ceramic systems. The (x) $\text{Pb}(\text{Mg}_{1/3}\text{Nb}_{2/3})\text{O}_3$ - $(1-x)$ $\text{Pb}(\text{Zr}_{0.52}\text{Ti}_{0.48})\text{O}_3$ (when $x = 0, 0.1, 0.3, 0.5, 0.7, 0.9,$ and 1.0) ceramics are prepared from respective starting materials by a conventional mixed-oxide method. A combination of the Knoop and Vickers indentation techniques is employed to determine the mechanical properties of the ceramics. It is found that the Vickers hardness of the ceramics varies between 5.28 and 7.75 GPa while the Young's modulus values range from 65.9 to 99.6 GPa. The fracture toughness of 2.03 to 3.42 $\text{MPa}\cdot\text{m}^{1/2}$ is obtained from the ceramics tested. In general, it is observed that the mechanical properties of the ceramic systems are largely controlled by those of PMN ceramics.

Key words: PMN-PZT ceramics, Mixed-oxide method, Mechanical properties

INTRODUCTION

With distinct characteristics, lead magnesium niobate ($\text{Pb}(\text{Mg}_{1/3}\text{Nb}_{2/3})\text{O}_3$ or PMN) and lead zirconate titanate ($\text{Pb}(\text{Zr}_{1-x}\text{Ti}_x)\text{O}_3$ or PZT) ceramics have been employed extensively in different types of actuator and transducer applications (Cross, 1987; Xu, 1991). As a prototypic relaxor ferroelectric, PMN has advantages of having very high dielectric constant and broader operating temperature range, especially over the room temperature range, as a consequence of the diffuse paraelectric-ferroelectric phase transition which takes place in the vicinity of room temperature. In addition, as a result of their unique microstructural features, PMN ceramics exhibit low loss and non-hysteretic characteristics. However, the PMN ceramics have relatively low electromechanical coupling coefficients as compared to PZT. On the contrary to PMN, PZT ceramics have been utilized more in actuator and transducer applications due to their high electromechanical coupling coefficients near the morphotropic phase boundary (MPB) (Cross, 1987; Xu, 1991; Abe et al., 2000). However, PZT ceramics are fairly lossy as a result of their hysteretic behavior. This makes them unsuitable for applications that require high delicacy and reliability. Furthermore, PZT ceramics normally have very high Curie temperature (T_c) in the vicinity of 400°C . Usually, many applications require that T_c is close to ambient temperature. Therefore, there is a general interest to reduce the T_c of PZT ceramics to optimize their uses. Forming a solid-solution of PZT and relaxor ferroelectrics has been one of the techniques employed to improve the properties of

ferroelectric ceramics. With the complementary features of PMN and PZT, it is of special interest to investigate a solid-solution of PMN-PZT ceramics which are expected to possess more desirable features than single-phase PMN and PZT (Ouchi et al., 1965; Ouchi, 1968; Xu, 1991).

However, most of earlier studies on PMN-PZT ceramics have been focused on processing, dielectric and electrical properties of the system. It is then of interest to examine the mechanical properties of the ceramic systems (Shilnikov et al., 1999; He et al., 2001; Stringfellow et al., 2002). The mechanical properties of the PMN-PZT systems require a special attention because these ceramics are usually used under an influence of stress in most of the actuator and transducer applications (Murty et al., 1992; Yoo et al., 1998). Thus, this study is undertaken to investigate for the first time the mechanical properties of the PMN-PZT ceramic systems.

MATERIALS AND METHODS

The $\text{Pb}(\text{Mg}_{1/3}\text{Nb}_{2/3})\text{O}_3$ - $\text{Pb}(\text{Zr}_{0.52}\text{Ti}_{0.48})\text{O}_3$ ceramics are prepared from PMN and PZT powders by a mixed-oxide method. Detailed procedures of each preparation step are described elsewhere (Yimnirun et al., 2003). Perovskite-phase PMN powders are obtained via a well-known columbite method (Swartz and Shrout, 1982). In this method, the magnesium niobate powders are first prepared by mixing starting MgO and Nb_2O_5 powders and then calcined to form a so-called columbite powder (MgNb_2O_6). The columbite powders are subsequently ball-milled with PbO . After another calcination process, a perovskite-phase PMN is formed. PZT powders, on the other hand, are prepared by a more conventional mixed-oxide method. With a more conventional oxide-mixing route, PZT powders are prepared from PbO , ZrO_2 , and TiO_2 starting powders. These powders are ball-milled and later calcined to yield the PZT powders. The (x) $\text{Pb}(\text{Mg}_{1/3}\text{Nb}_{2/3})\text{O}_3$ - $(1-x)$ $\text{Pb}(\text{Zr}_{0.52}\text{Ti}_{0.48})\text{O}_3$ (when $x = 0, 0.1, 0.3, 0.5, 0.7, 0.9,$ and 1.0) ceramic systems are prepared from the starting PMN and PZT powders by a mixed-oxide method at various calcining conditions. The mixed powders are pressed hydraulically to form disc-shaped pellets, 15 mm in diameter and 2 mm thick. The pellets are sintered in a covered alumina crucible filled with PZ powders to prevent lead loss. For optimization purpose, the sintering temperature is varied between 1000°C - 1300°C , depending upon the compositions.

The densities of the sintered ceramics are measured by Archimedes method from the specimens weighed in air, in water and the density of water. The phase formations of the sintered specimens are studied by XRD technique. The microstructure analyses are undertaken by a scanning electron microscopy (SEM: JEOL Model JSM 840A). Grain size is determined from SEM micrographs by a linear intercept method. A combination of the Knoop and the Vickers indentation techniques (Microhardness Testers: Model Matsuzawa MXT- α and Model Galileo Microscan-2) is used to determine various mechanical properties of the ceramics, such as the Vickers hardness (HV), the Young's modulus (E) and the fracture toughness (K_{Ic}).

With the indentation techniques used, the Vickers hardness (HV) is calculated from $(1.18185 \times 10^{10} \times P)/d^2$ relation, where P is the weight of the indenter used and d is the average

length of the indented surface. Using the Knoop indentation technique, the Young's modulus (E) is determined from $\alpha \cdot HK \cdot (0.1407 - (b/a))$ relation, where α is the constant (0.45), HK is the Knoop hardness in GPa unit, and (b/a) is the ratio of the diagonal lengths of the indented surface. Finally, the fracture toughness (K_{Ic}) is determined from the microhardness tester (model Galileo Microscan-2) experiment and the K_{Ic} is then calculated from $0.016(E/HV)^{1/2}(P/C^{3/2})$ relation, where E and HV are the values obtained earlier, P is the indenter weight (in a unit of MPa), and C is the length of the fracture (in a unit of meter) (Meechoowas, 2002).

RESULTS AND DISCUSSION

The phase formation behavior of the sintered ceramics is revealed by an XRD method. The XRD patterns, shown in Figure 1, indicate that PZT ceramic is identified as a material with a perovskite structure having tetragonal symmetry (JCPDS card no.33-784) while PMN ceramic is a perovskite material with a cubic symmetry (JCPDS card no. 81-0861). All PMN-PZT ceramic composites exhibit pseudocubic crystal structure, as reported in previous investigations (Ouchi et al., 1965; Ouchi, 1968). However, some impurity phases ($Pb_2Nb_2O_7$ and MgO) are also observed in the ceramics with $x > 0.1$. These impurities phases are believed to precipitate mostly on the surface areas of the specimens (Park et al., 2001). Further XRD investigation at different depths of the specimens reveals that the impurities diminish in the interior areas of the specimens.

The SEM micrographs of $x(\text{PMN} - (1-x)(\text{PZT})$ ceramics, sintered at 1150°C , are shown in Figure 2. Clearly, the morphology of the grains is composition-dependent and shows mixed features of the two end-members. PZT and PMN ceramics exhibit more uniform microstructure than those of the PMN-PZT ceramics. It should be noted that some of the grains are observed to be in irregular shapes with some open pores. This is a result of a Pb-loss during the sintering process. Grains of the PMN ceramics are mostly in spherical-like shape, while those of the secondary pyrochlore phase ($Pb_2Nb_2O_7$) exhibit a pyramidal morphology. The SEM micrographs also reveal that the PMN-PZT ceramics with $x = 0.1$ and $x = 0.3$ contain very small and loosely-bonded grains. This clearly suggests that the two compositions are not well sintered.

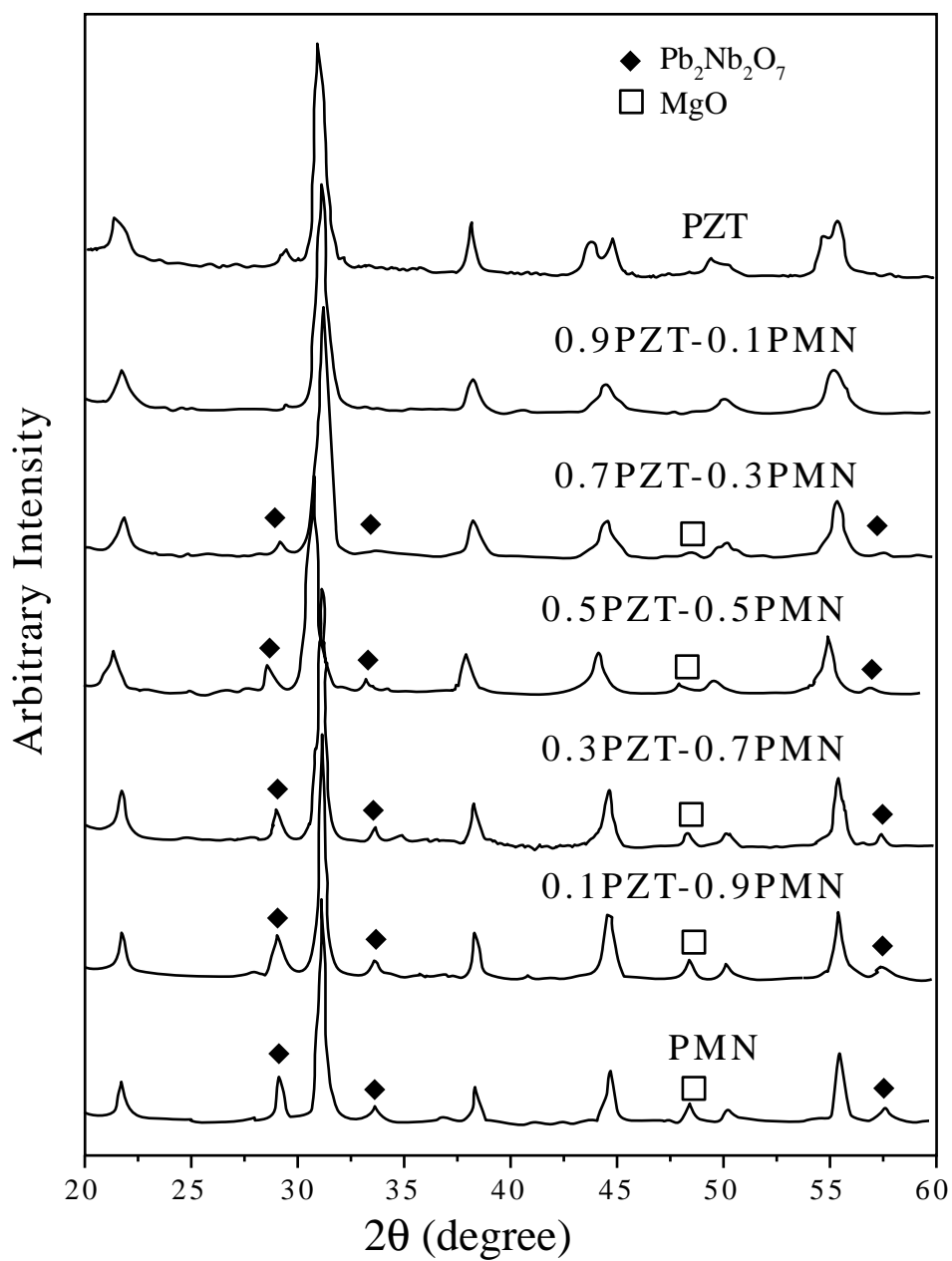


Figure 1. XRD patterns of $x \cdot \text{PMN} - (1-x) \cdot \text{PZT}$ ceramics.

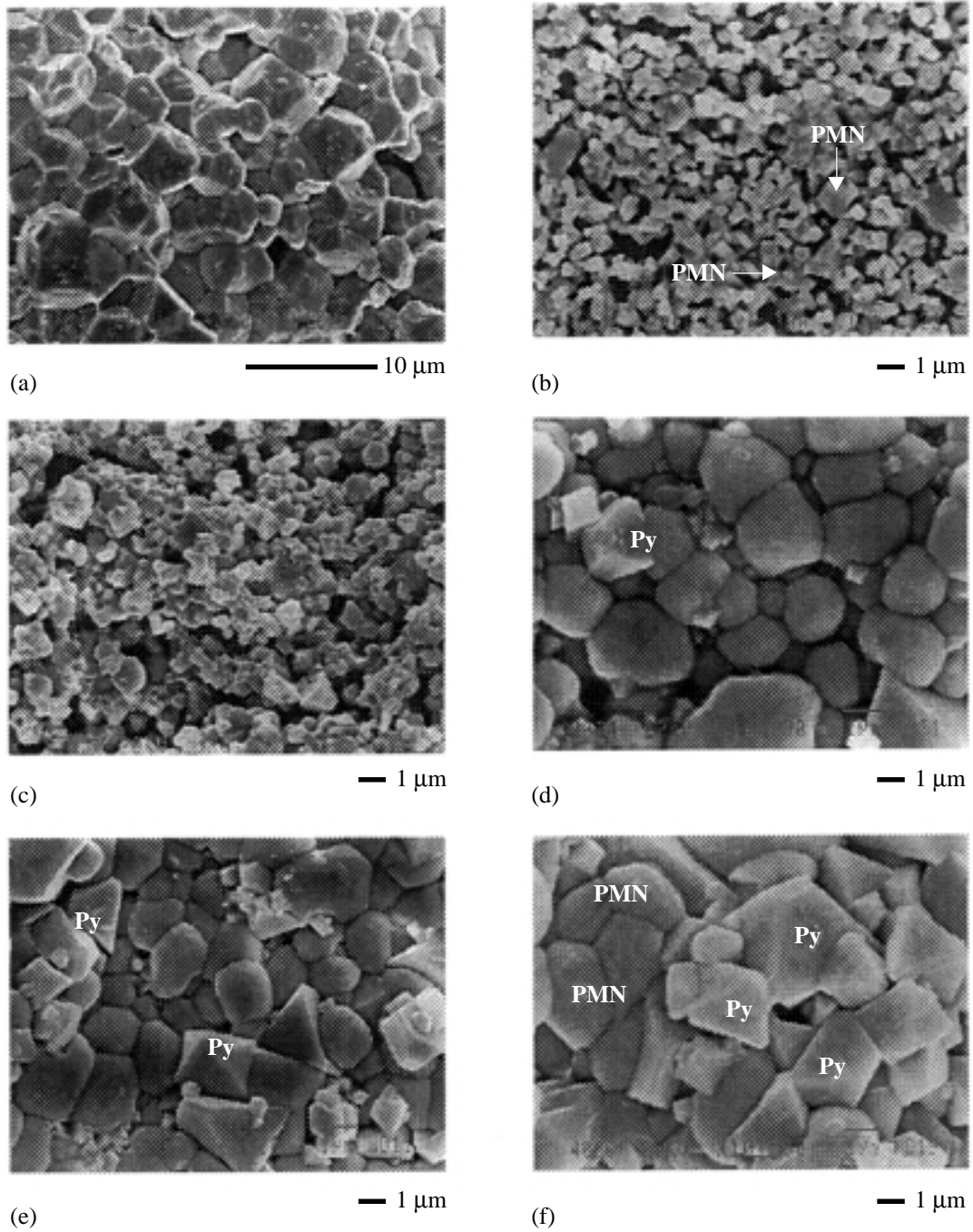


Figure 2. SEM micrographs of ceramics sintered at 1150°C: (a) PZT; (b) 0.1PMN-0.9PZT; (c) 0.3PMN-0.7PZT; (d) 0.7PMN-0.3PZT; (e) 0.9PMN-0.1PZT; and (f) PMN (Py indicates Pyrochlore Phase).

As listed in Table 1, the average grain size varies considerably from 1.40 μm to 5.23 μm . It should also be noted that the average grain size of all mixed compositions is much smaller than that of the end members. The reason for the smaller grain sizes is not clearly understood, but this may be a result of PMN's role as a grain-growth inhibitor in the PMN-PZT systems.

Table 1. Summary of physical data and optimum mechanical properties for a given composition of x-PMN - (1-x)·PZT ceramics.

Composition	Density (g/cm^3)	Average Grain Size (μm)	Vickers Hardness (HV) (GPa)	Young's Modulus (E) (GPa)	Fracture Toughness (K_{Ic}) ($\text{MPa}\cdot\text{m}^{1/2}$)
PZT	7.59 ± 0.11	5.23	5.28 ± 0.49	65.9 ± 2.6	2.48 ± 0.12
0.5PZT-0.5PMN	7.86 ± 0.05	1.90	7.16 ± 0.28	82.4 ± 9.4	3.42 ± 0.26
0.3PZT-0.7PMN	7.87 ± 0.07	1.40	7.28 ± 0.33	99.6 ± 6.1	3.03 ± 0.29
0.1PZT-0.9PMN	7.90 ± 0.09	1.50	7.13 ± 0.37	89.3 ± 9.4	2.03 ± 0.24
PMN	7.82 ± 0.06	3.25	7.75 ± 0.18	84.3 ± 5.6	2.84 ± 0.10

Table 1 also summarizes the optimum mechanical properties for a given composition of x-PMN - (1-x)·PZT ceramics, evaluated by the Knoop and the Vickers indentation techniques. It should be mentioned that the mechanical properties of 0.1PMN- 0.9PZT and 0.3PMN- 0.7PZT ceramics are not available. As a result of their low densities, the mechanical properties of the 0.1PMN- 0.9PZT and 0.3PMN- 0.7PZT ceramics are not quantifiable. The Vickers hardness (HV) of PMN is found to be highest (7.75 GPa) among the ceramics tested. It is also of interest to observe that all the mixed compositions exhibit much larger hardness value (7.13-7.16 GPa) than that of pure PZT (5.28 GPa). This clearly indicates that PMN addition enhances the hardness of ceramics in PMN-PZT system, as the Vickers hardness value increases from 5.28 GPa in PZT ceramic to 7.28 GPa in 0.7PMN-0.3PZT ceramic. This could be attributed to the facts that hardness is a material's surface property and that there are some mechanically-hard materials (MgO and $\text{Pb}_2\text{Nb}_2\text{O}_7$) precipitating on the surfaces of the mixed compositions, as described in earlier discussions.

Similarly, the Young's modulus (E) of the PMN and PMN-PZT ceramics (varying between 82.4 GPa and 99.6 GPa) is significantly higher than that of PZT ceramic, which is measured to be 65.9 GPa. However, an addition of PZT into PMN-PZT system results in an increase in the Young's modulus of the mixed compositions until the trace off is observed in 0.5PZT-0.5PMN ceramic when the density begins to drop due to loss of PbO during the sintering process. The reason for this observation is somewhat linked to the density of these ceramics. As seen in Table 1, ceramics with higher density possess comparatively higher value of the Young's modulus.

The fracture toughness (K_{Ic}) of these ceramics is more difficult to understand because it depends on many factors, for instance grain size and morphology, crystal structure and phase

and pore size and distribution. However, it is generally observed that except for the 0.9PMN-0.1PZT composition, the fracture toughness of the mixed compositions (3.42 and 3.03 MPa·m^{1/2} for 0.5PMN-0.5PZT and 0.7PMN-0.3PZT, respectively) is higher than that of PMN and PZT ceramics, reported as 2.84 and 2.48 MPa·m^{1/2}). This could very well be a result of a fracture-inhibition effect by the mechanically- and physically- different components in the mixtures.

Generally, it can be stated that the mechanical properties of the ceramic systems are largely controlled by those of PMN ceramics. It is also noticeable that PMN ceramics are mechanically-superior to PZT ceramics. Finally, it is of interest to observe that some of the ceramic systems exhibit better mechanical properties than those of the single-phase PMN or PZT. Intuitively, this can be attributed to a composite nature of the mixtures, in which some of the properties are enhanced by the presence of inclusions.

CONCLUSIONS

In this study, the (x) Pb(Mg_{1/3}Nb_{2/3})O₃ - (1-x) Pb(Zr_{0.52}Ti_{0.48})O₃ (when x = 0, 0.1, 0.3, 0.5, 0.7, 0.9, and 1.0) ceramic systems are prepared by a conventional mixed-oxide method at various processing conditions. Perovskite-phase PMN and PZT powders, prepared by a columbite route and a mixed-oxide route, respectively, are used as starting powders for the PMN-PZT ceramic systems preparation. Density measurements, XRD and SEM studies and mechanical properties tests indicate that PMN phase show very important roles in controlling the properties of the ceramic systems. Finally, it is clearly shown that the mechanical properties, e.g., Vickers hardness, Young's modulus and fracture toughness of the ceramics with mixed compositions are generally better than those of the end members.

ACKNOWLEDGEMENTS

The authors would like to express their gratitude for financial supports from the Thailand Research Fund (TRF) and Professor Dr. Nuth Bhamornprave's Foundation, Faculty of Science, Chiang Mai University.

REFERENCES

- Abe, Y., T. Yanagisawa, K. Kakegawa, and Y. Sasaki. 2000. Piezoelectric and dielectric properties of solid solution of PbZrO₃-PbTiO₃-Pb(Mg_{1/3}Nb_{2/3})O₃ system prepared by wet-dry combination method. *Solid State Commun.* 113 : 331-334.
- Cross, L.E. 1987. Relaxor ferroelectrics. *Ferroelectrics.* 76 : 241-267.
- He, L.X., M. Gao, C.E. Li, W.M. Zhu, and H.X. Yan. 2001. Effects of Cr₂O₃ addition on the piezoelectric properties and microstructure of PbZr_xTi_y(Mg_{1/3}Nb_{2/3})_{1-x-y}O₃ ceramics. *J. Euro. Ceram. Soc.* 21 : 703-709.
- Meechoowas, E. 2002. Compositions and mechanical property relationships in lead zirconate titanate/lead magnesium niobate ceramics. M.S. Thesis. Chiang Mai University, Chiang Mai, Thailand.

- Murty, K.V.R., S.N. Murty, K.C. Mouli, and A. Bhanumathi. 1992. Domain orientation and piezoelectric properties of Ag doped PMN-PZT ceramics. Proceeding of the IEEE International Symposium on Applications of Ferroelectrics. 1 : 144-147.
- Ouchi, H. 1968. Piezoelectric properties and phase relation of $\text{Pb}(\text{Mg}_{1/3}\text{Nb}_{2/3})\text{O}_3$ - PbTiO_3 - PbZrO_3 ceramics with barium or strontium substitutions. J. Am. Ceram. Soc. 51(3) : 169-176.
- Ouchi, H., K. Nagano, and S.J. Hayakawa. 1965. Piezoelectric properties of $\text{Pb}(\text{Mg}_{1/3}\text{Nb}_{2/3})\text{O}_3$ - PbTiO_3 - PbZrO_3 solid solution ceramics. J. Am. Ceram. Soc. 48(12) : 630-635.
- Park, J.H., K.H. Yoon, and D.H. Kang. 2001. Dielectric and electrical properties of preferentially (111) oriented Zr-rich $0.1\text{Pb}(\text{Mg}_{1/3}\text{Nb}_{2/3})\text{O}_3$ - $0.9\text{Pb}(\text{Zr}_x\text{Ti}_{1-x})\text{O}_3$ thin films by chemical solution deposition, Thin Solid Films. 396 : 84-89.
- Shilnikov, A.V., A.V. Sopot, A.I. Burkhanov, and A.G. Luchaninov. 1999. Dielectric response of electrostrictive (1-x)PMN-xPZT ceramics. J. Euro. Ceram. Soc. 19 : 1295-1297.
- Stringfellow, S.B., S. Gupta, C. Shaw, J.R. Alcock, and R.W. Whatmore. 2002. Electrical conductivity control in uranium doped PbZrO_3 - PbTiO_3 - $\text{Pb}(\text{Mg}_{1/3}\text{Nb}_{2/3})\text{O}_3$ pyroelectric ceramics. J. Euro. Ceram. Soc. 22 : 573-578.
- Swartz, S.L. and T.R. Shrout. 1982. Fabrication of perovskite lead magnesium niobate. Mater. Res. Bull. 17 : 1245-1250.
- Xu, Y.H. 1991. Ferroelectric materials and their applications, University of California Los Angeles, North Holland.
- Yimnirun, R., S. Ananta, E. Meechoowas, and S. Wongsanmai. 2003. Effect of uniaxial stress on dielectric properties of lead magnesium niobate-lead zirconate titanate ceramics. J. Phys. D: Appl. Phys. 36 : 1615-1619.
- Yoo, J. H., H.S. Yoon, Y.H. Jeong, and C.Y. Park. 1998. Piezoelectric characteristics of PMN-PZT ceramics for piezoelectric transformer. Proceeding of the IEEE Ultrasonic Symposium. 981-984.